

Metal-Enhanced Fluorescence from Silver–SiO₂–Silver
Nanoburger StructuresYongxia Zhang,[†] Lynda N. Mandeng,[†] Nina Bondre,[†] Anatoliy Dragan,[†] and Chris D. Geddes^{*,‡}[†]Institute of Fluorescence and [‡]Institute of Fluorescence and Department of Chemistry and Biochemistry,
University of Maryland Baltimore County, 701 East Pratt Street, Baltimore, Maryland 21202

Received May 5, 2010

Multilayers of nanoburger structures of silver island films–SiO₂–silver island films (SIFs–SiO₂–SIFs) were used as substrates to study the fluorescence of close-proximity fluorophores. Compared to single-layered SIFs, multilayer nanoburgers exhibit several distinctive properties including a significantly enhanced fluorescence intensity, decreased lifetimes, and increased fluorophore photostability by simply varying the dielectric layer thickness while the SIF layer is kept constant. Finite-difference time-domain (FDTD) calculations show that the maximum electric field intensity can be tuned by varying the distance between the silver particles. Enhanced fluorescence emission coupled with a reduced fluorophore lifetime suggests that both an electric field and plasmon-coupling component are the underlying mechanisms for nanoburger-based metal-enhanced fluorescence (MEF). This tunable multilayer nanoburger structure holds great potential for applications in biology, microscopy, imaging, and biomedical research, given the current uses of MEF.

1. Introduction

Fluorescence detection is an important tool in medical diagnostic high-throughput screening, microscopy, and biotechnology.^{1–5} Although fluorescence spectroscopy displays exquisite sensitivity,^{2,6,7} the detection limit is usually limited by the quantum yield of the fluorophore (label), the autofluorescence of the sample, and the photostability of the fluorophores, which are fundamentally far-field fluorescence properties.⁸ In this regard, metallic nanostructures^{9–12} have been used to modify the spectral properties of fluorophores favorably and to alleviate some of their more classical photophysical

far-field constraints.^{13–23} The use of fluorophore–metal near-field interactions has been termed metal-enhanced fluorescence (MEF) by Geddes.²⁴ To date, MEF from plasmonic nanostructured materials such as silver,^{25,26} gold,²⁷ copper,²⁸ zinc,²⁹ chromium,³⁰ nickel,³¹ tin,³² and iron³³ has been observed in our laboratory. In this regard,

*To whom correspondence should be addressed. Tel: +1-410-576-5723. Fax: +1-410-576-5722. E-mail: geddes@umbc.edu.

(1) Alfano, R. R.; Tang, G. C.; Pradhan, A.; Lam, W.; Choy, D. S. J.; Opher, E. Fluorescence-spectra from cancerous and normal human-breast and lung tissues. *IEEE J. Quantum Electron.* **1987**, *23*, 1806–1811.

(2) Chance, R. R.; Miller, A. H.; Prock, A.; Silbey, R. Fluorescence and energy-transfer near interfaces - complete and quantitative description of eu+3-mirror systems. *J. Chem. Phys.* **1975**, *63*, 1589–1595.

(3) Choi, S.; Choi, E. Y.; Kim, D. J.; Kim, J. H.; Kim, T. S.; Oh, S. W. A rapid, simple measurement of human albumin in whole blood using a fluorescence immunoassay (I). *Clin. Chim. Acta* **2004**, *339*, 147–156.

(4) Cullum, M. E.; Lininger, L. A.; Schade, S. Z.; Cope, S. E.; Ragain, J. C., Jr.; Simonson, L. G. Diagnosis of militarily relevant diseases using oral fluid and saliva antibodies: fluorescence polarization immunoassay. *Mil. Med.* **2003**, *168*, 915–921.

(5) Davidson, R. S.; Hilchenbach, M. M. The use of fluorescent-probes in immunochemistry. *Photochem. Photobiol.* **1990**, *52*, 431–438.

(6) Andersson, H.; Baechli, T.; Hoehli, M.; Richter, C. Autofluorescence of living cells. *J. Microsc.* (Oxford, U. K.) **1998**, *191*, 1–7.

(7) Enderlein, J.; Ruckstuhl, T.; Seeger, S. Highly efficient optical detection of surface-generated fluorescence. *Appl. Opt.* **1999**, *38*, 724–732.

(8) Thompson, R. B. *Fluorescence Sensors and Biosensors*. CRC Press: Boca Raton FL, 2006.

(9) Chowdhury, S.; Bhethanabotla, V.; Sen, R. Silver-copper alloy nanoparticles for metal enhanced luminescence. *Appl. Phys. Lett.* **2009**, *95*, 131115.

(10) Stefani, F.; Vasilev, K.; Bocchio, N.; Stoyanova, N.; Kreiter, M. Surface-plasmon-mediated single-molecule fluorescence through a thin metallic film. *Phys. Rev. Lett.* **2005**, *94*, 023005.

(11) Garrett, S.; Smith, L.; Barnes, W. Fluorescence in the presence of metallic hole arrays. *J. Mod. Opt.* **2005**, *52*, 1105.

(12) Praharaj, S.; Ghosh, S.; Nath, S.; Kundu, S.; Panigrahi, S.; Basu, S.; Pal, T. Size-selective synthesis and stabilization of gold organosol in CnTAC: Enhanced molecular fluorescence from gold-bound fluorophores. *J. Phys. Chem. B* **2005**, *109*, 13166.

(13) Stranik, O.; McEvoy, H.; McDonagh, C.; MacCraith, B. Plasmonic enhancement of fluorescence for sensor applications. *Sens. Actuators, B* **2005**, *107*, 148.

(14) Aroca, R.; Kovacs, G. J.; Jennings, C. A.; Loutfy, R. O.; Vincett, P. S. Fluorescence enhancement from Langmuir–Blodgett monolayers on silver island films. *Langmuir* **1988**, *4*, 518–521.

(15) Chen, Y.; Munechika, K.; Ginger, D. S. Dependence of fluorescence intensity on the spectral overlap between fluorophores and plasmon resonant single silver nanoparticles. *Nano Lett.* **2007**, *7*, 690–696.

(16) Cheng, P. P.; Silvester, D.; Wang, G.; Kaluzhny, G.; Douglas, A.; Murray, R. W. Dynamic and static quenching of fluorescence by 1–4 nm diameter gold monolayer-protected clusters. *J. Phys. Chem. B* **2006**, *110*, 4637–4644.

(17) Croce, A. C.; Ferrigno, A.; Vairetti, M.; Bertone, R.; Freitas, I.; Bottioli, G. Autofluorescence properties of isolated rat hepatocytes under different metabolic conditions. *Photochem. Photobiol. Sci.* **2004**, *3*, 920–926.

(18) Doron, A.; Katz, E.; Willner, I. Organization of au colloids as monolayer films onto ito glass surfaces: Application of the metal colloid films as base interfaces to construct redox-active monolayers. *Langmuir* **1995**, *11*, 1313–1317.

(19) Kawasaki, M.; Mine, S. Enhanced molecular fluorescence near thick Ag island film of large pseudotubular nanoparticles. *J. Phys. Chem. B* **2005**, *109*, 17254–17261.

(20) Malicka, J.; Gryczynski, I.; Geddes, C. D.; Lakowicz, J. R. Metal-enhanced emission from indocyanine green: A new approach to in vivo imaging. *J. Biomed. Opt.* **2003**, *8*, 472–478.

(21) Dostalek, J.; Knoll, W. Biosensors based on surface plasmon-enhanced fluorescence spectroscopy. *Biointerphases* **2008**, *3*, FD12.

(22) Gersten, J. I. *Theory of Fluorophore–Metallic Surface Interactions*. Springer: New York, 2004; Vol. 8, pp 197–221.

(23) Kasry, A.; Knoll, W. Long range surface plasmon fluorescence spectroscopy. *Appl. Phys. Lett.* **2006**, *89*, 101106.

(24) Geddes, C. D.; Lakowicz, J. R. Metal-enhanced fluorescence. *J. Fluoresc.* **2002**, *12*, 121–129.

(25) Aslan, K.; Malyn, S. N.; Geddes, C. D. Angular-dependent metal-enhanced fluorescence from silver colloid-deposited films: opportunity for angular-ratio-metric surface assays. *Analyst* **2007**, *132*, 1112–1121.

(26) Aslan, K.; Lakowicz, J. R.; Szmanski, H.; Geddes, C. D. Metal-enhanced fluorescence solution-based sensing platform. *J. Fluoresc.* **2004**, *14*, 677–679.

(27) Aslan, K.; Malyn, S. N.; Geddes, C. D. Metal-enhanced fluorescence from gold surfaces: angular dependent emission. *J. Fluoresc.* **2007**, *17*, 7–13.

(28) Zhang, Y.; Aslan, K.; Prevote, M. J. R.; Geddes, C. D. Metal-enhanced fluorescence from copper substrates. *Appl. Phys. Lett.* **2007**, *90*, 173116.

(29) Aslan, K.; Prevote, M. J. R.; Zhang, Y.; Geddes, C. D. Metal-enhanced fluorescence from nanoparticulate zinc films. *J. Phys. Chem. C* **2008**, *112*, 18368–18375.

(30) Pribik, R.; Aslan, K.; Zhang, Y.; Geddes, C. D. Metal-enhanced fluorescence from chromium nanodeposits. *J. Phys. Chem. C* **2008**, *112*, 17969–17973.

(31) Zhang, Y.; Dragan, A.; Geddes, C. D. Near-infrared metal-enhanced fluorescence using nickel nanodeposits. Submitted to *J. Phys. Chem. C* **2009**.

(32) Zhang, Y.; Dragan, A.; Geddes, C. D. Metal-enhanced fluorescence from tin nanostructured surfaces. *J. Appl. Phys.* **2010**, 024302.

(33) Zhang, Y.; Padhyay, A.; Sevilleja, J. E.; Guerrant, R. L.; Geddes, C. D. Interactions of the fluorophores with iron nanoparticles: Metal-enhanced fluorescence. *J. Phys. Chem. C* **2010**, *114*, 7575.

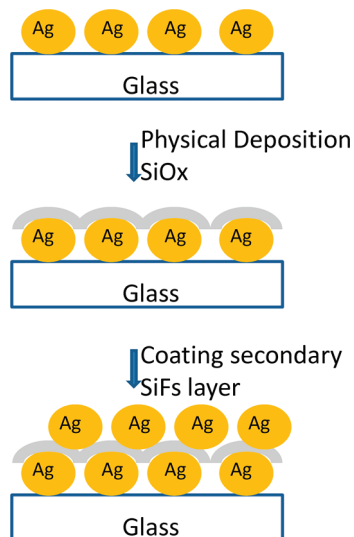


Figure 1. Process of nanoburger surface preparation.

silver island films (SIFs) have been a popular substrate used for applications of MEF for fluorophores emitting in the visible wavelength region. However, these studies have for the most part been focused on one SIF layer.^{14,34,35}

In this article, we present experimental and theoretical electric field simulations of a new type of modified SIF—nanoburger structures—to test whether it is suitable for MEF applications. SIF nanoburger structures were fabricated by combining wet chemical silver deposition with the thermal vapor deposition of SiO₂ onto glass microscope slides, which were subsequently characterized by optical absorption spectroscopy and atomic force microscopy (AFM) techniques. The resultant layered structures are likened to hamburger geometry and thus are called nanoburgers. Significantly enhanced fluorescence emission was observed when fluorophores were positioned close to the nanoburger structures. In addition, we have observed a shorter fluorescence lifetime for fluorophores, which in accordance with current MEF theory suggests that both an enhanced electric field and a plasmon-coupling component underpin the mechanism for fluorescence enhancement close to the SIF—SiO₂ multilayered nanoburger structures.

2. Results and Discussion

The morphology of a series of SIF nanoburger structures was first studied using AFM. Figure 2 shows the morphology of SIFs: SIFs—10 nm SiO₂ and SIFs—10 nm SiO₂—SIFs. The irregular size of 125 nm Ag particles with a surface roughness around 32.5 nm (Figure 2b) can be seen for the first layer of the SIF films (Figure 2a). After the deposition of SiO₂ (Figure 2b), the film surface is smoother with a roughness of around 25.7 nm. When the second layer of SIFs was deposited onto SiO₂, a fairly unstructured silver film with a roughness of around 37.9 nm and a particle size of around 125 nm was again observed.

Figure 3b shows the extinction spectra of the SIF nanoburger structure (SIFs—5 nm SiO₂—SIFs) and SIFs—5 nm SiO₂. It can be seen that the SIF nanoburger structure has a much larger optical density of the extinction spectra with a maximum wavelength that is red-shifted (410 nm) as compared to a single layer of SIFs—5 nm SiO₂ (390 nm). This increase in extinction is attributed to the

higher cumulative optical density of two layers of SIFs compared with one layer of SIFs, and the subsequent wavelength shift is attributed to the near-field refractive index change between individual SIFs with the SiO₂ isolation layer. The absorption of fluorescein on the SIF nanoburger structure (SIFs—5 nm SiO₂—SIFs) and SIFs—5 nm SiO₂ is shown in Figure 3c using SIFs—5 nm SiO₂ and SIFs—5 nm SiO₂—SIFs films as the backgrounds, respectively. The fluorophore has a much larger absorbance on SIFs—5 nm SiO₂—SIFs as compared to that on SIFs—5 nm SiO₂ alone, which has the same maximum absorbance wavelength of FITC (Figure 3c inset). For nanoburger structures with different SiO₂ thickness, we observed a similar extinction property where there are much larger extinction spectra as compared to that for a single layer of SIFs—*x* nm SiO₂. These effects can be explained as a result of the coupling of the molecular dipoles with the localized electromagnetic field of the metallic particle's surface plasmon resonance (localized plasmon resonance, LPR) in the ground state. In essence, conducting metallic particles can modify the free-space far-field absorption condition (observed in the absence of metal) in ways that increase the incident electric field, E_m , felt by the close proximity of near-field fluorophores.³⁶

To test the nanoburger substrate for potential applications in MEF, the fluorescence emission spectra of fluorescein in water on SIFs—SiO₂—SIFs films with different thickness of SiO₂ and on glass were recorded with excitation at 455 nm, and the spectra and enhancement factor (relative to a glass control) are compiled in Figure 4. From Figure 4f, it can be seen that the fluorescence of fluorescein is enhanced (~35 times) on both SIFs—7 nm SiO₂—SIFs and SIFs—10 nm SiO₂—SIFs, where the enhancement factor of the thickness of SIFs—7 nm SiO₂ is 20 and 14 times of SIFs—10 nm SiO₂. Also, we observed that the fluorescence enhancement factor (as compared to a plain glass control sample) increased as the SiO₂ thickness increased (from 2 to 10 nm) and decreased when the SiO₂ thickness reached ~15 nm. Also, the fluorescence enhancement factor from the nanoburger substrate is much larger than that of a single layer of SIFs without SiO₂,^{14,34,35,37} where the enhanced emission is facilitated by the close proximity of the fluorophore to the nanoburger layers (i.e., a near-field interaction). In this regard, it will be shown later in this article that this enhancement effect loosely correlates with the enhanced electric field component from the substrates as simulated using FDTD, suggesting that enhanced absorption contributes significantly to MEF.

The photostability (steady-state intensity decay) of fluorescence on SIFs—10 nm SiO₂ and SIFs—10 nm SiO₂—SIFs (i.e., nanoburger) was also measured. Figure 5 shows the fluorescence emission as a function of time, with excitation at 455 nm and observed through a 500 nm long-pass filter. The relative intensities of the plots reflect that more detectable photons can be observed per unit time from the SIFs—10 nm SiO₂—SIFs film as compared to the number that can be observed per unit time from the SIFs—SiO₂ (a control sample not containing the silver), where the integrated areas under the plots are proportional to the photon flux from the respective surfaces. By additionally adjusting the laser power to match the same initial steady-state intensities of the samples at time $t = 0$, the FITC on SIFs—10 nm SiO₂—SIFs can be seen to be more photostable (Figure 5). Similar findings were observed for the other SIFs—SiO₂ geometries studied. This finding of enhanced photostability subsequently implies that the fluorescence lifetime from the SIFs—10 nm SiO₂—SIFs will be shorter than on the SIFs—10 nm SiO₂ film, with the fluorophore in essence spending less time

(34) Garoff, S.; Weitz, D. A.; Gramila, T. J.; Hanson, C. D. Optical-absorption resonances of dye-coated silver-island films. *Opt. Lett.* **1981**, *6*, 245–247.

(35) Zhang, Y.; Dragan, A.; Geddes, C. D. Wavelength-dependence of metal-enhanced fluorescence. *J. Phys. Chem. C* **2009**, *113*, 12095–12100.

(36) Lakowicz, J. R. Radiative decay engineering: Biophysical and biomedical applications. *Anal. Biochem.* **2001**, *298*, 1–24.

(37) Aslan, K.; Badugu, R.; Lakowicz, J. R.; Geddes, C. D. Metal-enhanced fluorescence from plastic substrates. *J. Fluoresc.* **2005**, *15*, 99–104.

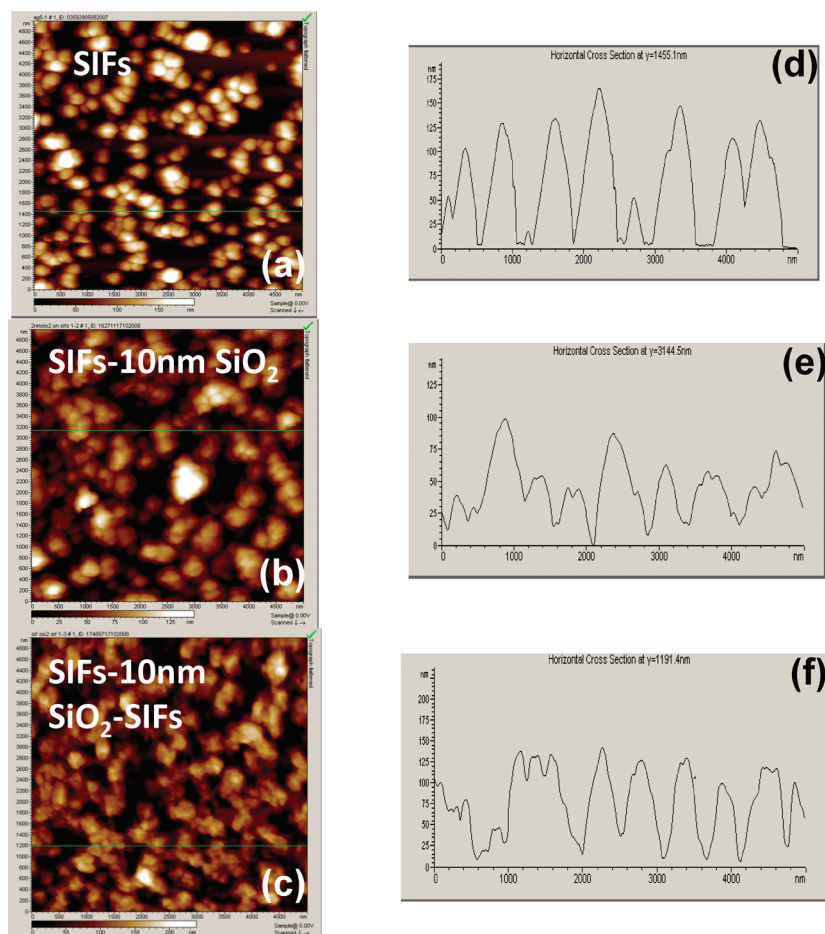


Figure 2. AFM images of SIFs (a), SIFs–10 nm SiO₂ (b), and nanoburgers (SIFs–10 nm SiO₂–SIFs) (c). The respective line scans of the AFM images are shown in d–f. The roughness is 32.5 nm for SIFs, 25.7 nm for SIFs–10 nm SiO₂, and 37.9 nm for SIFs–10 nm SiO₂–SIFs.

on average in an excited state because of the fast nonradiative energy transfer to the SIFs–10 nm SiO₂–SIFs, and therefore is less prone to photodestruction (i.e., is more photostable). In terms of a substrate for analytical chemistry applications, a higher photon flux (counts per unit time) will invariably increase the fluorescence detectability from the surfaces. We have also measured the time-resolved intensity decays of fluorescein (fluorescence lifetimes) in close proximity to SIFs and nanoburger structures (data shown in Table 1) using the time-correlated single photon counting technique. The respective lifetimes were calculated from those decays using nonlinear least-squares impulse reconvolution analysis. We see both a reduced amplitude lifetime ($\langle\tau\rangle$ on SIFs–7 nm SiO₂ and SIFs–7 nm SiO₂–SIFs is 3.29 and 2.21 ns, respectively) and mean lifetimes (τ_{mean} on SIFs–7 nm SiO₂ and SIFs–7 nm SiO₂–SIFs is 4.76 and 2.89 ns and $\langle\tau\rangle$ on SIFs–10 nm SiO₂ and SIFs–10 nm SiO₂–SIFs is 3.30 and 2.21 ns, respectively, and τ_{mean} on SIFs–10 nm SiO₂ and SIFs–10 nm SiO₂–SIFs is 4.68 and 3.0 ns, respectively) as compared to the glass control sample (τ_{mean} on glass is 5.02 ns and $\langle\tau\rangle$ on glass is 4.71 ns). These findings of reduced fluorophore lifetimes are consistent with our previously reported findings for nanosecond decay time fluorophores sandwiched between single-layer silver nanostructures, similarly suggesting that the radiating

plasmon model^{38–40} is a suitable description of the nanoburger fluorescence-enhancement mechanism. In this description, the lifetime of the fluorophore–metal system is reduced because of faster, more efficient fluorophore–plasmon coupling, followed in turn by coupled-system emission, with the plasmon in essence radiating the coupled quanta through the scattering component of its extinction spectrum.

Subsequently, we suggest two complementary effects for the observed fluorescence enhancement: (i) surface plasmons can radiate coupled fluorescence efficiently and (ii) an enhanced absorption or electric field facilitates enhanced emission. Because enhanced electromagnetic fields in close proximity to metal nanoparticles are the basis for the increased system absorption in MEF, we have additionally calculated the electric field distributions for nanoburger nanostructures with various SiO₂ thickness using FDTD calculations (Figure 6). FDTD calculations show that the maximum electric field of the nanoburger structure increases with the thickness of SiO₂ and then decreases when the thickness of SiO₂ exceeds 5 nm, similar to that observed experimentally (i.e. Figure 4).⁴¹ However, the values are not identical, which is simply explained by the differences between empirical and theoretical data. These collective observations not only are helpful for creating surface architectures for optimized

(38) Aslan, K.; Leonenko, Z.; Lakowicz, J. R.; Geddes, C. D. Annealed silver-island films for applications in metal-enhanced fluorescence: Interpretation in terms of radiating plasmons. *J. Fluoresc.* **2005**, *15*, 643–654.

(39) Lakowicz, J. R. Radiative decay engineering 5: Metal-enhanced fluorescence and plasmon emission. *Anal. Biochem.* **2005**, *337*, 171–194.

(40) Drexhage, K. H. Influence of a dielectric interface on fluorescence decay time. *J. Luminesc.* **1970**, *1/2*, 693–701.

(41) Kummerlen, J.; Leitner, A.; Brunner, H.; Ausseneegg, F. R.; Wokaun, A. Enhanced dye fluorescence over silver island films - analysis of the distance dependence. *Mol. Phys.* **1993**, *80*, 1031–1046.

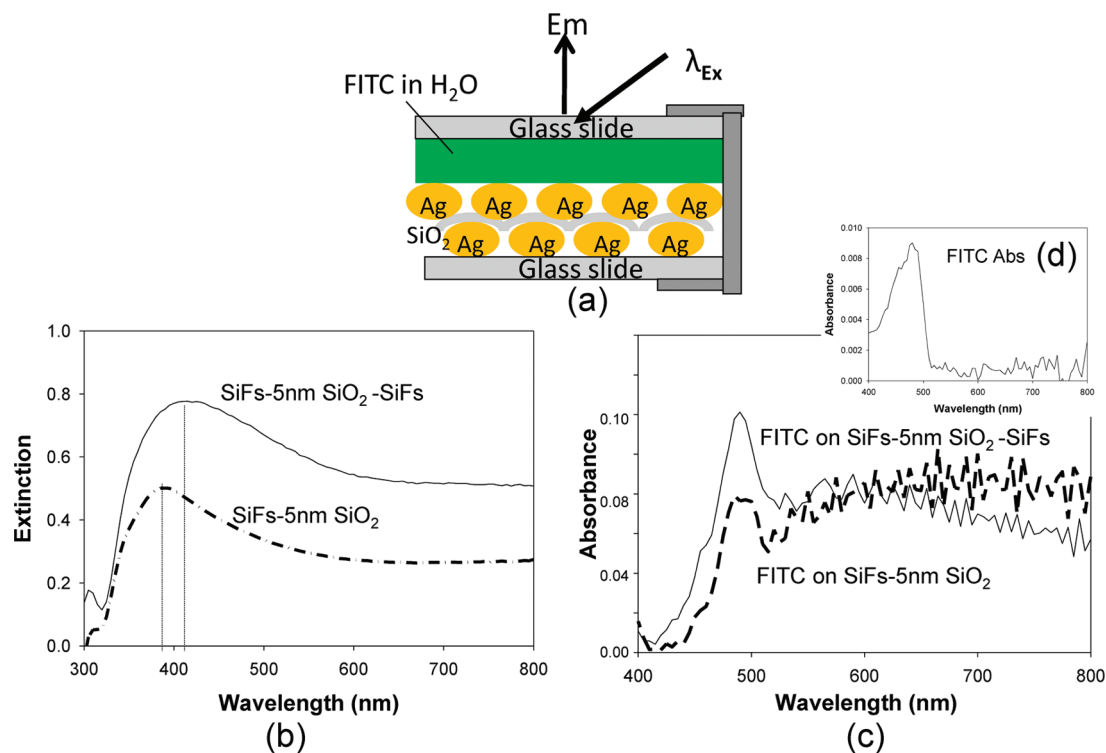


Figure 3. Schematic for FITC solutions sandwiched between one glass and one nanoburger slide (a). Absorbance spectra of SiFs–5 nm SiO₂–SiFs and SiFs–5 nm SiO₂–SiFs (b). Absorbance spectra of FITC on SiFs–5 nm SiO₂ and on SiO₂–5 nm SiO₂–SiFs (c). Absorbance spectra of a FITC solution measured in a cuvette (d).

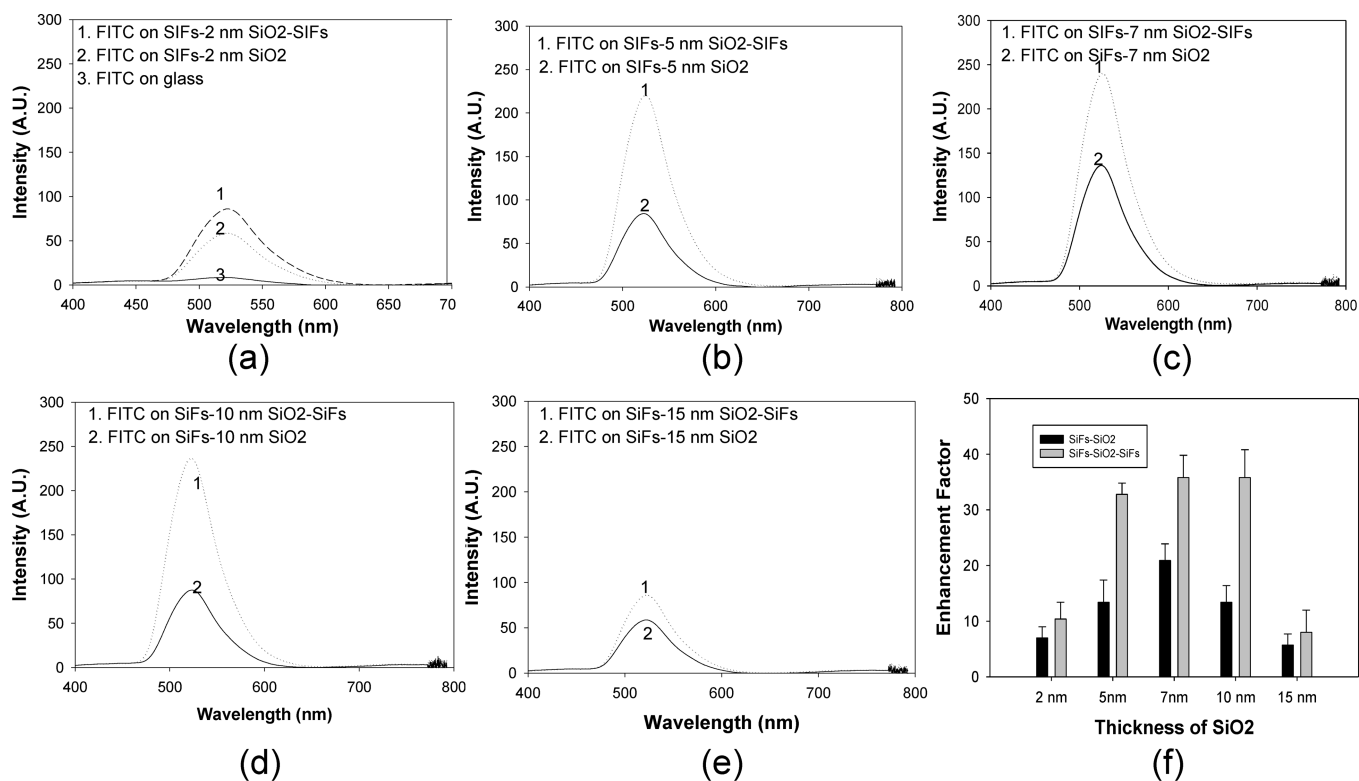


Figure 4. Fluorescence spectra and enhancement factor of FITC solutions sandwiched between one glass slide and one nanoburger slide with different SiO₂ thicknesses: (a) 2 nm SiO₂, (b) 5 nm SiO₂, (c) 7 nm SiO₂, (d) 10 nm SiO₂, and (e) 15 nm SiO₂. Excitation: 455 nm.

MEF but also are helpful in our laboratories where we continue to develop a unified plasmon–fluorophore theory/description.

2.1. Two Mechanisms in MEF. In this article, we have shown that a fluorophore close to the SiFs nanoburger structures

can display enhanced absorption, as shown experimentally in Figure 3, which has been further modeled in Figure 6 with a modest correlation between both sets of data. In this regard, the enhanced absorption of the fluorophore does not lend itself to a

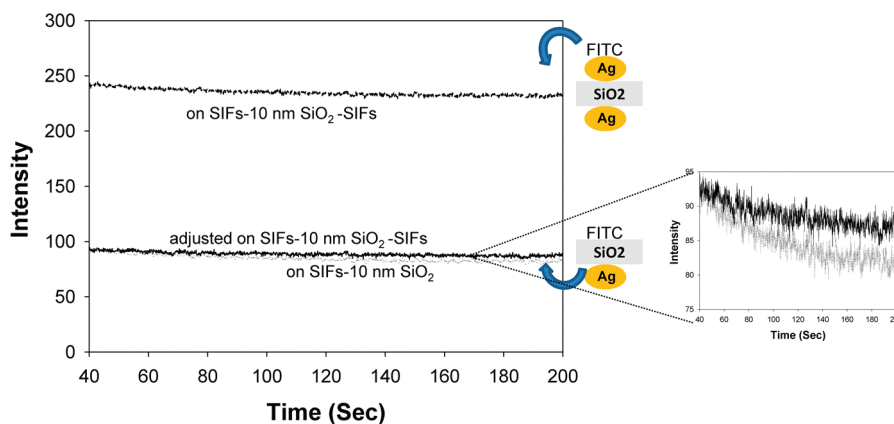


Figure 5. Emission intensity vs time for FITC on SIFs–10 nm SiO₂ and SIFs–10 nm–SiO₂–SIFs with the laser power adjusted to give the same initial steady-state fluorescence intensity as observed on SIFs–10 nm SiO₂ (bottom curves).

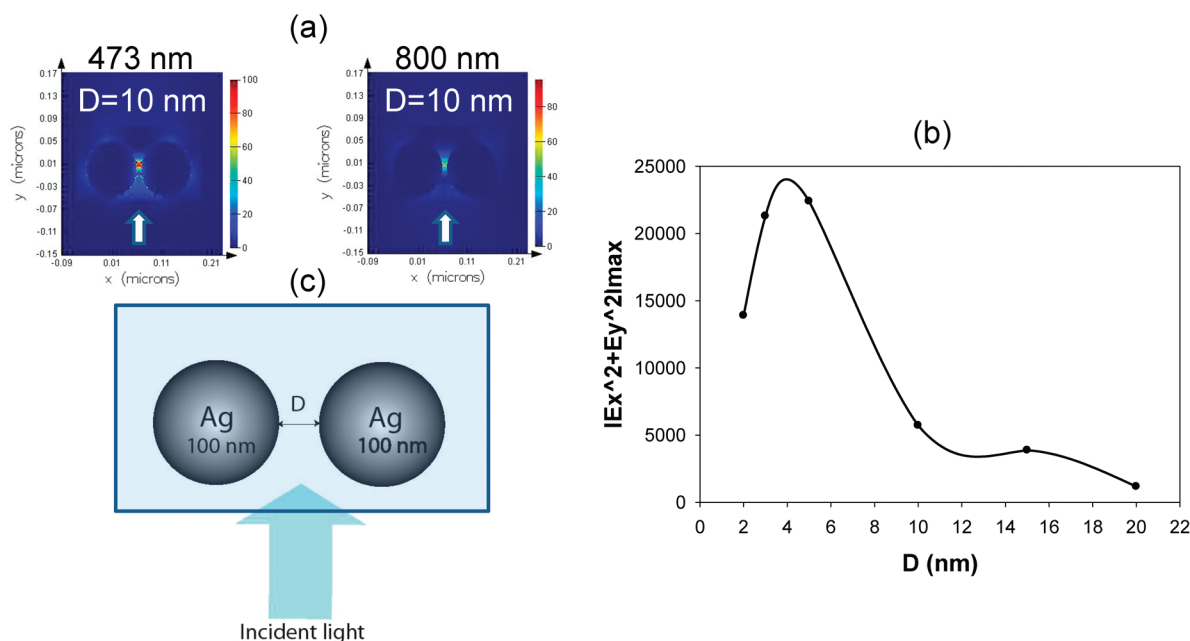


Figure 6. Dependence of the E -field intensity on the distance ($D = 10$ nm) between NPs of incident light at 473 nm and 800 nm (a). Images of the 2D E -field distribution around silver NPs for incident-light wavelengths of 473 nm. (Arrows show the direction of incident light injection in the simulation.) $|E_x^2 + E_y^2|_{\max}$ was calculated along D (b). Cartoon showing the setup for the FDTD calculations of the near-field intensity that were made for 100-nm-diameter silver NPs with a background refractive index of 1.5 (SiO₂) (c).

reduced fluorescence lifetime, which we have attributed to an additional MEF mechanism, the so-called plasmon coupling component, described in numerous reports by our laboratory.³⁸ For fluorophores under the far-field condition (i.e., more than 1 wavelength away from the nanoburger structures), the fluorescence quantum yield and lifetime are described by the classical equations

$$Q_0 = \frac{\Gamma}{\Gamma + k_{nr}} \quad (1)$$

$$\tau_0 = \frac{1}{\Gamma + k_{nr}} \quad (2)$$

where Γ is the far-field fluorophore radiative rate. k_{nr} represents the nonradiative rates, Q_0 is the quantum yield, and τ_0 is the free-space lifetime. From these two equations, we can readily see that as one modifies the k_{nr} rates, such as by adding a quencher, both the quantum yield and lifetime change in unison.

However, for fluorescein solutions close to the nanoburger structures we see enhanced emission, Q_m , coupled to a reduced lifetime, τ_m , which is quite different from the traditional free-space conditions (i.e., eqs 1 and 2)

$$Q_m = \frac{\Gamma + \Gamma_m}{\Gamma + \Gamma_m + k_{nr}} \quad (3)$$

$$\tau_m = \frac{1}{\Gamma + \Gamma_m + k_{nr}} \quad (4)$$

where τ_m , Q_m , and Γ_m are the metal-modified system lifetimes, quantum yields (overall brightness), and system radiative rates, respectively.

From Figure 5, we note a better fluorescein photostability that we attribute to the reduced fluorophore lifetime close to metal (confirmed by time-resolved measurements, Table 1), with the fluorophore spending on average less time in an excited state prior

Table 1. Fluorescence Lifetime Analysis of FITC in Water and on SIF Nanoburger Deposits Measured Using Time-Domain Fluorometry^a

	T_1 (ns)	A_1 (%)	T_2 (ns)	A_2 (%)	$\langle\tau\rangle$ (ns)	$\bar{\tau}$ (ns)	χ^2
FITC–glass	4.44	95.37	10.27	4.63	4.71	5.02	1.05
FITC–SIFs	4.02	92.37	8.27	7.63	4.34	4.63	1.05
FITC–SIFs–7 nm SiO ₂	2.61	91.25	10.4	8.75	3.29	4.76	1.02
FITC–SIFs–7 nm SiO ₂ –SIFs	1.94	95.33	7.77	4.67	2.21	2.89	0.92
FITC–SIFs–10 nm SiO ₂	2.60	90.25	10.1	9.75	3.30	4.68	1.04
FITC–SIFs–10 nm SiO ₂ –SIFs	1.91	94.53	7.71	5.47	2.21	3.00	0.95

^a $\bar{\tau}$ is the mean lifetime, and $\langle\tau\rangle$ is the amplitude-weighted lifetime.

to its deactivation to the ground state and thus having less time for photochemical excited-state reactions (i.e., it is more photo-stable). The presence of both an enhanced absorption and a reduced lifetime suggests two complementary mechanisms for fluorescence enhancement, which have been reported numerous times for single metal surface deposits.³⁸

3. Conclusions

In this article, we report the first observation of MEF from multiple layers of SIFs–SiO₂–SIFs, which we have called nanoburger substrates because of the similarity to hamburger-type geometry. We observed significantly enhanced fluorescence intensity, decreased lifetimes, and increased photostability when fluorophores were placed in close proximity to the multilayer nanoburger structure as compared to single-layered SIFs, which hitherto have been the most widely used substrate in MEF studies. Furthermore, the enhancement factor can be tuned by changing the SiO₂ thickness between the SIFs layers, which is a result of the

changing e-field between the particles. We have subsequently suggested both an enhanced electric field, E_m , and a plasmon-coupling component to be the mechanisms for the observed fluorescence enhancement, similar to that for substrates made from silver, copper, and gold nanoparticles alone, as previously reported by our laboratory.

Acknowledgment. The authors would like to thank the Institute of Fluorescence and UMBC (University of Maryland Baltimore County) for salary support.

Supporting Information Available: Preparation of nanoburger substrates for metal-enhanced fluorescence (MEF) measurements. Preparation of the sandwich format sample. Fluorescence lifetime analysis. Optical spectroscopy. Atomic force microscopy (AFM). FDTD calculations. This material is available free of charge via the Internet at <http://pubs.acs.org>.